Phase Morphology and Clay Distribution of Poly(trimethylene terephthalate)/Polypropylene/ Montmorillonite Nanocomposites

Mei-Ling Xue, Peng Li

Key Lab of Rubber-Plastics, Ministry of Education, Qingdao University of Science and Technology, Qingdao 266042, People's Republic of China

Received 1 October 2008; accepted 24 January 2009
DOI 10.1002/app.30417
Published online 27 May 2009 in Wiley InterScience (www.interscience.wiley.com).

ABSTRACT: Poly(trimethylene terephthalate) (PTT)/polypropylene (PP) blend nanocomposites were prepared by melt mixing of PTT, PP, and organically modified clay. The phase morphologies of the PTT/PP nanocomposites and the distribution of the clay in the nanocomposites were investigated using scanning electron microscopy, transmission electron microscopy (TEM), and wide angle X-ray diffraction. When PP is the dispersed phase, the domain size of the PP phase is decreased significantly with increasing the clay content from 0 to 5 wt %. In contrast, when PTT is the dispersed phase, the dimension of the PTT phase is a little larger in the presence of 2 wt % clay compared with the case of without clay. TEM observations indicate that the clay is mainly distributed at the phase interfaces along the phase borderlines. In addition, some intercalated clay tactoids (multilayer particles) are observed in the PTT matrix whereas no discernable clay particles can be found in the PP phase, indicating that the affinity of clay with PTT is higher than with PP. In the presence of 5 wt % PP-graft-maleic anhydride, the phase morphology is much finer, and most clay is exfoliated and distributed at the phase interfaces forming phase borderlines in polygonal shape. © 2009 Wiley Periodicals, Inc. J Appl Polym Sci 113: 3883–3890, 2009

Key words: poly(trimethylene terephthalate); nanocomposites; clay dispersion

INTRODUCTION

Polymer materials are required to meet the more and more versatile applications at the present time. To synthesize new polymeric materials is both time consuming and much costly. However, blending or alloying polymers with different properties is a straightforward and relatively inexpensive method of creating new polymer materials by synergistic combinations of the desirable properties of the constituent components.[1–3] Another way to broaden the application window of the homopolymer materials is to make polymer/layered silicate nanocomposites, which combines the advantages of the organic and inorganic materials.[4–6] It is well established that the intercalated/exfoliated microstructures of the organoclay in the polymer matrix endow the polymer with enhanced mechanical properties, improved thermal stability, low gas barrier properties, and increased electronic conductivity.

In the recent years, with the many possible of combinations the advantages offered by blends and polymer/clay nanocomposites, there is a growing interest in the polymer/polymer/nanoclay ternary composites.[7–12] Due to the different affinities of the clay with the two polymers, the clay may selectively distribute in one phase domains, two phase domains or at the interfaces. As a result, its effects on the phase morphologies and the properties of the resultant composites were diversified.[9–11] Li and Shimizu[8] found that the original sea-island morphology of the 40/60 ABS/PA6 blend was transformed into a cocontinuous structure with the addition of 2 wt % organoclay. The phase size decreased significantly with increasing clay loading, and the clay was selectively distributed in the PA6 phase. Similarly, the domain size of the dispersed poly(ethylene-ran-propylene) rubber (EPR) phase in the PA6 matrix decreased dramatically even if when a small amount of clay was added,[9] whereas the dispersed PA6 domain did not decrease with increasing the clay content up to 2 wt %. By using poly(*p*-phenylene sulfide)/polyamide66 blends as an example, Zou et al.[10] demonstrated that clay could not only affect the phase morphology of the immiscible polymer blends, but also showed the locking effects on the phase morphology. Tang et al.[11] reported that the different blending sequences influenced the dispersibility of the clay in the PP/PA6 blends.

Poly(trimethylene terephthalate) (PTT) is a newly commercialized crystalline polymer with growing applications in fibers, films, and engineering plastics.[13–15] However, the low heat distortion

Correspondence to: M.-L. Xue (meilingxue2003@yahoo.com.cn).

temperature, low melt viscosity, and pronounced brittleness of unreinforced PTT at low temperature have restricted its use as a desirable engineering plastic. Some of these deficiencies could be improved by developing PTT composites or blends with suitable polymers in which it retains its excellent properties. PP is one of the most high volume polymers with good processability, relatively high performance and low cost. The PTT/PP blends combine the desire properties of the two homopolymers, whereas its tensile strength and modulus are lower than that of PTT,[16] which can be improved by preparing PTT/PP/nanoclay composites. In this study, the PTT/PP/MMT nanocomposites were first prepared by melt mixing. The dispersion and distribution of the clay in the PTT blend nanocomposites were investigated.

EXPERIMENTAL

Materials

Clear PTT, with the trade name Corterra CP509201, was supplied by the Shell Chemical Company, WV. The polymer had an intrinsic viscosity of 0.92 dL/g, measured in a 60/40 mixture of phenol and tetrachloroethane at 30°C. Polypropylene (PP), injection grade, with the trade name SJ-170T and a melt flow rate of 28 g/10 min at 230°C, was purchased from Honam petrochemical Corp., Korea. The clay used in this study is an organically modified montmorillonite, with the trade name Cloisite® 25A, was purchased from Southern Clay Products. PP-graft-maleic anhydride (PP-g-MAH), with the trade name Umex 1010, was purchased from Sanyo Chemical Industry K. K., Japan. The weight-average molecular weight of PP-g-MAH is 30,000, which is measured by GPC method. Before melt processing, PTT was dried at 140°C for at least 12 h in a vacuum oven to minimize the hydrolytic degradation of the melts. Cloisite 25A, PP, and PP-g-MAH were dried at 100°C, 80°C and 80°C, respectively, for 2 h in the vacuum oven. All the components were thoroughly mixed before melt mixing.

Preparation of blends

Melt blending was conducted using a Haake Rheocord 9000. The mixing temperature was 245°C and the mixing time was 10 min. The screw speed was 60 rpm. After the mixing was finished, the blends were rapidly quenched in ice water to freeze the morphologies of the melt states. They were then dried at room temperature under vacuum before further measurements.

Characterization

The samples for scanning electron microscopy (SEM) observation were fractured in liquid nitrogen. The fracture surface morphologies of the blends and nanocomposites were examined using a field-emission scanning electron microscope (FE-SEM) Hitachi S-4700.

Transmission electron microscopy (TEM) observations were carried out to examine the micromorphology of the samples. Ultrathin sections of the blends and nanocomposites were microtomed at room temperature using an Ultratome (Model MT-6000, Du Pont Company) equipped with a diamond knife. The ultra-thin sections were put on copper grids and then observed using a JEOL JSM-2000EX TEM under an acceleration voltage of 200 kV.

Wide angle X-ray diffraction measurements were performed on a Japan Rigaku D/max 2500 m with Cu Kα radiation ($\lambda = 0.154$ nm) at room temperature. The accelerating voltage was 40 kV and a current of 100 mA. Data were collected with a step size of 0.02° from $2\theta = 1°$–10°.

RESULTS AND DISCUSSION

Phase morphology

Figure 1 shows the SEM images of the PTT/PP blends with or without clay. All the images show typical sea-island morphologies. For the 80/20 PTT/PP blend, the spherical PP domains disperse in the PTT matrix because of the small level volume fraction of PP. The interface is smooth, indicating the poor adherence between the PTT phase and the PP phase. With the addition of 0.55 wt % clay, the PP domain size decreases noticeably. When the clay content increases from 0.55 to 5 wt % the dimension of the PP phase decreases dramatically, and then a slow dimension decrease is observed as the clay content increases up to 7 wt %. This result indicates that the clay plays an important role in reducing the domain size of the dispersed PP phase in the PTT matrix, and this reduction of the PP domain size is as a function of the clay content. These phenomena are also observed in other immiscible blends.[7–12] As the clay content is increased, the fracture surface also shows significant changes. Both the dispersed PP spheres and the holes in the matrix are well shaped when the clay content is in the range of 0–2 wt %, whereas they are rough and irregular when the clay content is up to 5 wt % or above. This indicates that the dispersion-coalescence process of the PP phase in the matrix is interfered severely due to the introduction of clay, and this interference is not only exhibited as the size reduction of the dispersed phase but also as the rough interfaces between the dispersed and the matrix phases. Moreover, the

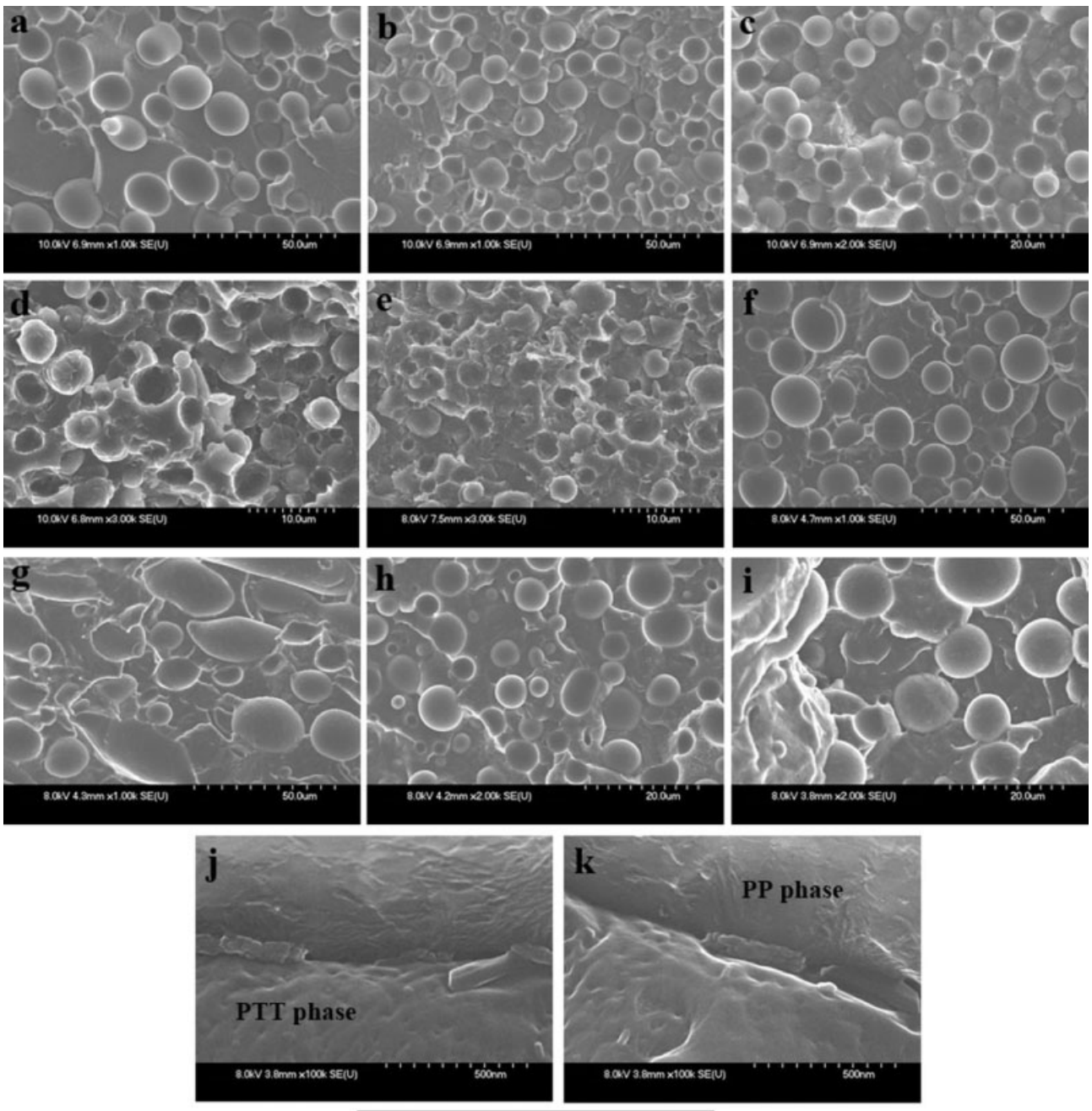

Figure 1 SEM micrographs of the effects of clay and its content on the phase morphology of the PTT/PP blends. a, PTT/PP=80/20; b, PTT/PP/clay = 80/20/0.5%; c, PTT/PP/clay = 80/20/2%; d, PTT/PP/clay = 80/20/5%; e, PTT/PP/clay=80/20/7%; f:PTT/PP=40/60; g, PTT/PP/clay = 40/60/2%; h, PTT/PP = 30/70; i, PTT/PP/clay = 30/70/2%; j, PTT/PP/clay = 30/70/2%; k, PTT/PP/clay=30/70/2%.

interference is more severely with increasing in the clay content. It is noteworthy that, from the TEM micrographs of a–e, there is no improvement in the interface adherence is observed during the reduction development of the PP domain size with the clay content. This confirms that the size reduction of the dispersed PP phase is not due to the compatibilization effect of clay on the blends,[9] but is due to the interference of clay on the dispersion-coalescence process of the PP phase.

When PTT is the dispersed phase, i.e., at the composition of 30/70/2 wt % PTT/PP/clay, the effect of the clay on the phase morphology is opposite. Typical SEM images are shown as images f–i in Figure 1. The dispersion of the PTT phase is not finer but coarser in the presence of 2 wt % clay. Obviously, the different effects of the clay on the phase morphologies of the blends are related to which polymer is the matrix phase; moreover, it implies that the clay exhibits different distributions and may be

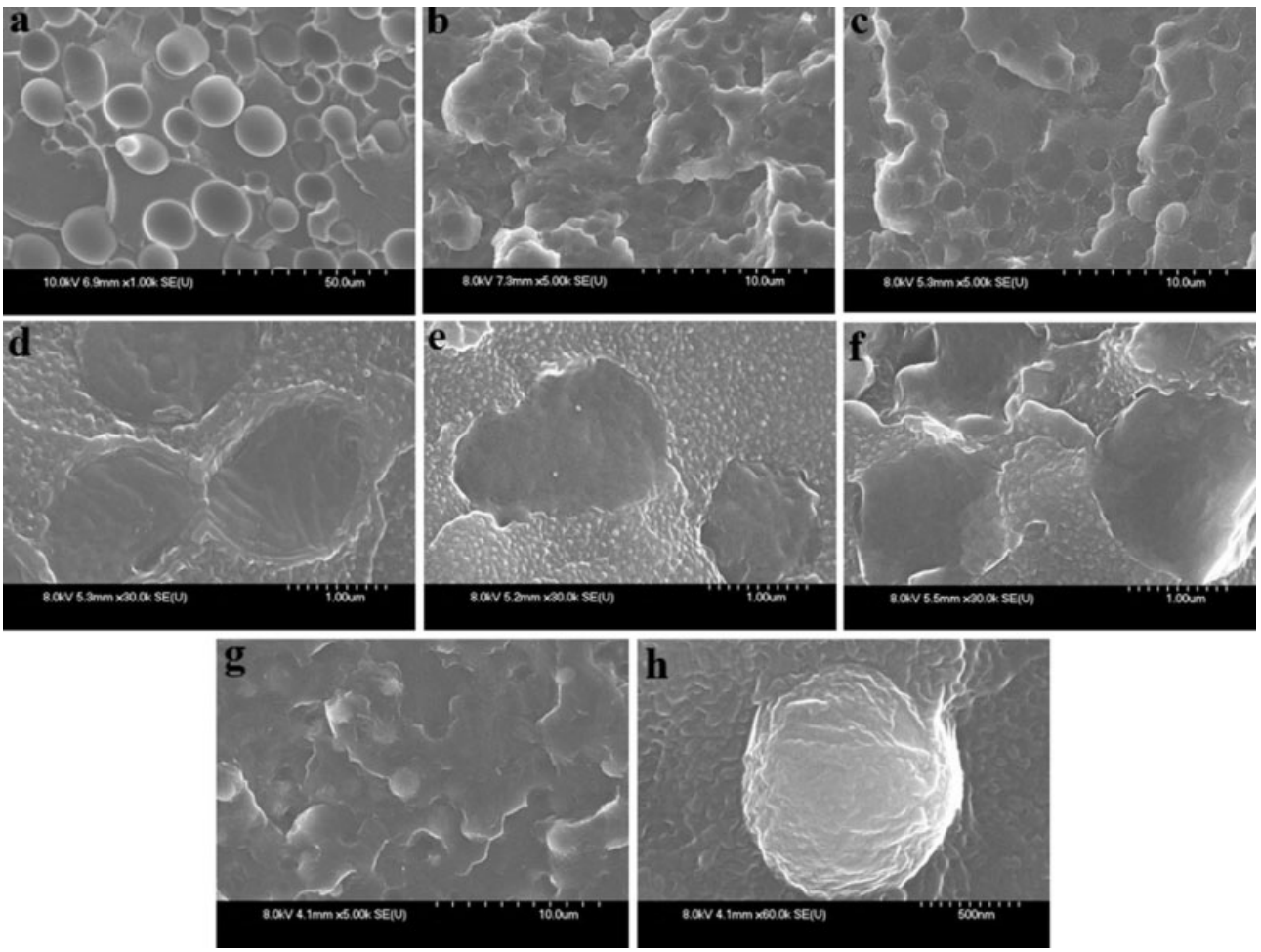

Figure 2 SEM micrographs of the effects of 5 wt % PP-g-MAH on the phase morphology of the PTT/PP/clay blend nanocomposites. a, PTT/PP = 80/20; b, PTT/PP/PP-g-MA = 80/20/5%; c, PTT/PP/PP-g-MA/clay = 80/20/5%/0.5%; d, PTT/PP/PP-g-MA/clay = 80/20/5%/0.5%; e, PTT/PP/PP-g-MA/clay = 80/20/5%/2%; f, PTT/PP/PP-g-MA/clay = 80/20/5%/5%; g, PTT/PP/PP-g-MA/clay = 30/70/5%/2%; h, PTT/PP/PP-g-MA/clay = 30/70/5%/2%.

different dispersions in the two polymer phases. Images j and k show the presence of clay conglomerations locating at the interfaces along the phase borders. Some nanodispersed clay particles are noticed on the surfaces of the PTT spheres, but no clay particles are found in the PP matrix.

To compare the effect of compatibilizer with that of clay on the phase morphologies of the PTT/PP blends, the freeze fracture surfaces of the PP-g-MAH compatibilized PTT/PP blend and PTT/PP blend nanocomposites were investigated, as shown in Figure 2. Comparing images a and b, it can be seen that, by the addition of 5 wt % PP-g-MAH, the domain size of the dispersed PP phase decreases significantly to ~1 μm, and the PP particles are dispersed uniformly in the PTT matrix with excellent interface adherence. With the addition of 0.55 wt % clay further (images c and d), a slightly increase in dimension of the PP particles is noticed. It implies that part of PP-g-MAH combined with clay and hence its amount which functioned as compatibilizer is decreased. The holes left by removing of the PP particles during the freeze fracture are observed with protuberant interfacial walls against the matrix. As the clay content increased further, the phenomena are disappeared, as shown in images e and f. The contour lines of the holes are not round circles but in irregular shapes, which indicates that the dispersion-coalescence process of the PP phase is disturbed by clay at higher content. Likewise, when PTT is the dispersed phase, as shown images g and h in Figure 2, the compatibility between the PTT phase and the PP phase is improved significantly in the presence of PP-g-MAH, which is similar to the case of the 80/20 PTT/PP blend. The PTT spheres are dispersed uniformly in the PP matrix with excellent adherence, and a clear interface layer in ~50 nm thickness is noticed from image h. Figure 2

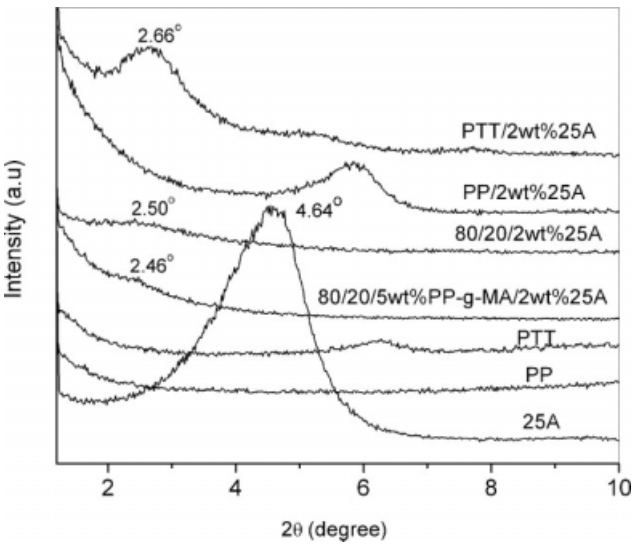

Figure 3 WAXD patterns of clay (Closite 25A) itself, pure PTT, PP, and their nanocomposites as well as the PTT/PP/clay blend nanocomposites when PP is the dispersed phase.

shows that the mechanism of the clay's effect on the morphology of the blends is different from that of the compatibilizer's.

Clay dispersion and distribution in the PTT/PP/MMT nanocomposites

To investigate the mechanism of the morphological changes of the PTT/PP/clay nanocomposite with the clay content, it is necessary to consider the dispersion and distribution of clay in the blends. The level of intercalation in clay was determined by the measurement of the clay interlayer spacing (d_{001}) from the 2θ position of the clay (001) diffraction peak. Figure 3 shows the WAXD patterns of the clay (Cloisite 25A) itself, pure PTT, PP, and their nanocomposites. The clay content in this investigation was 2 wt % for all nanocomposites. The diffraction peak of the (001) reflections of the clay is at $2\theta = 4.64°$, which corresponds to d_{001} spacing of 1.90 nm. The characteristic peak of the clay in the PTT/clay nanocomposite shifted to a lower angle diffraction of $2\theta = 2.66°$, indicating that PTT was intercalated between the clay layers. In contrast, there is no discernable diffraction peaks at lower angles is noticed for the PP/clay nanocomposites, but there is a broad peak with considerable intensity appears at $2\theta \approx 5.9°$. This indicates that some clay layers were totally exfoliated in the PP matrix, and also, some clay layers collapsed during mixing because of the falling off of the clay modifiers from the clay interlayers owing to its low thermal stability and was responsible for this interlayer spacing reduction.[5] However, the characteristic diffraction of the (001) planes in the 80/20/clay nanocomposite, displayed an indistinct broad peak with low intensity at $2\theta = 2.50°$, indicating that the level of exfoliation is high and the clay shows a finer dispersion when PTT is the matrix phase. With the addition of 5 wt % PP-g-MAH further, the diffraction peak nearly disappears, suggesting that PP-g-MAH improves the dispersibility of the clay in the both polymers.

Figure 4 shows the WAXD patterns of the 30/70 PTT/PP and its nanocomposites. For the 30/70/clay nanocomposite, a broad peak exhibited at a higher angle of $2\theta = 3.62°$ in comparison with the PTT/clay nanocomposite. The presence of this broad peak suggests that the clay exhibits a wide distribution of interlayer spacing, which is probably related to a more heterogeneous intercalation in the 30/70/clay nanocomposite and part of clay is exfoliated. With the addition of 5 wt % PP-g-MAH further, a much smaller and indistinct diffraction peak at $2\theta = 2.92°$ is noticed, indicating that both the exfoliation of the clay and the intercalation of the polymers are enhanced.

Figure 5 shows the TEM micrographs of the blend nanocomposites with 2 wt % clay. Images a, b, and c are micrographs of the 80/20/2 wt % nanocomposite with different magnifications. The size and the dispersion of the dispersed PP domains are in agreement with those obtained from the SEM images. The clay, which is intercalated or partially exfoliated, mainly distributes along the phase borderlines, which is clearly shown in image c. The distribution characteristic of the clay implies that its surface hydrophobicity (or hydrophilicity) is between those of PTT and PP, which causes its transfer from the PTT and the PP

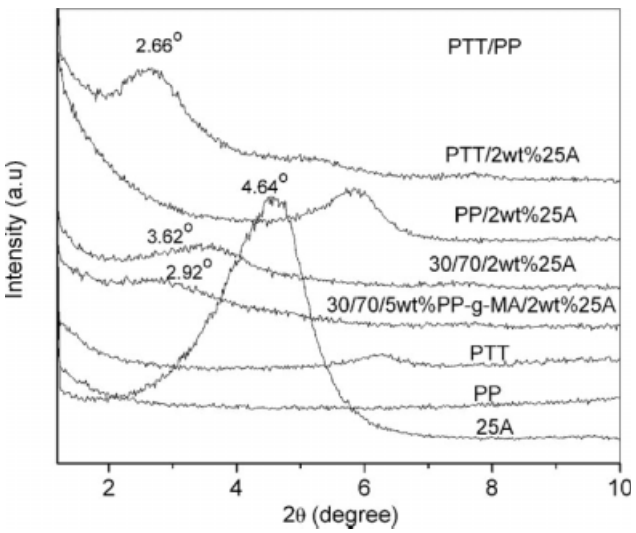

Figure 4 WAXD patterns of clay (Closite 25A) itself, pure PTT, PP, and their nanocomposites as well as the PTT/PP/clay blend nanocomposites when PTT is the dispersed phase.

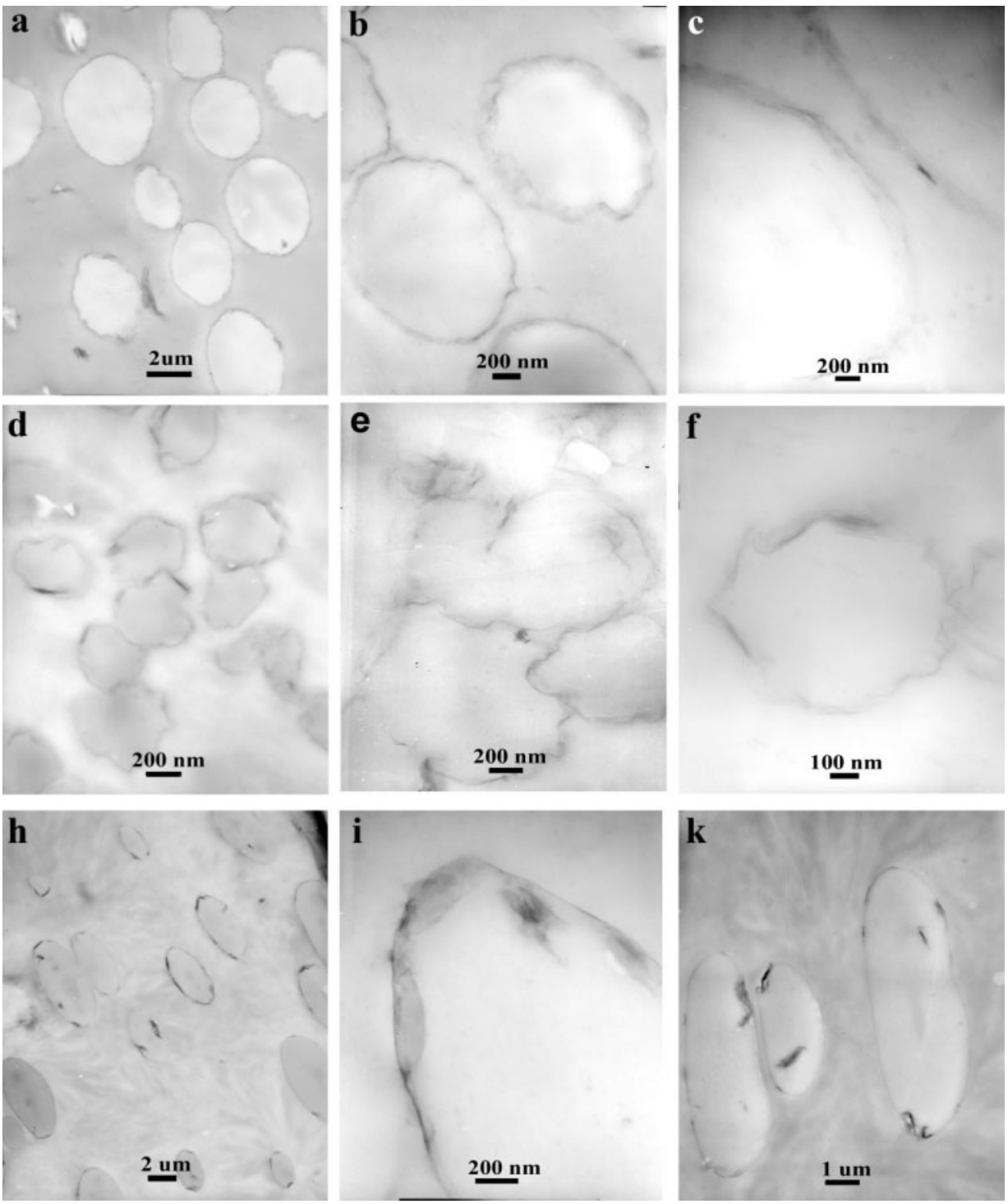

Figure 5 TEM micrographs of the PTT/PP blend nanocomposites at different magnifications. Sample compositions are as bellows: images a–c, 80/20/2 wt % clay; images d–f, 80/20/5 wt % PP-g-MAH/2 wt % clay; images h, i, and k, 30/70/2 wt % clay.

phases to the interface areas during the mixing process and be located preferentially at the interface areas as observed. In addition, a few intercalated clay tactoids (multilayer particles, image a) are observed in the PTT matrix, whereas no discernable clay particles are found in the PP domains. This indicates that the clay has slightly higher affinity with PTT than PP, and all the clay in the PP phase as well as part of clay in the PTT phase might have been transferred to the interface area during the mixing process.

When 5 wt % PP-g-MAH is added, the dimension of the PP domains decreases significantly, as shown

in images of d, e, and f in Figure 5, which is consistent with the phase size obtained from SEM. Moreover, most clay is exfoliated and distributes along the phase borderlines forming clay interfaces in several decade nanometers thickness. These results indicate that both the interfacial tensions between clay and the two polymers and the interfacial tension between the two polymeric phases are all decreased. As a result, the occurrences of the intercalation and exfoliation processes were facilitates. Furthermore, owing to the decreased PP domain size and the high aspect ratio of clay, the self-assembled clay at the interface forms phase borderlines in polygonal shape, and this is why the irregular PP domains are observed in Figure 2.

The morphology also shows changes for the cases of which PTT is the dispersed phase. The TEM images of h, i, and k in Figure 5 are the morphologies of the 30/70/2 wt % PTT/PP/clay nanocomposite. The dispersed PTT phase exhibits elongated domains or elliptical shapes in the PP matrix because of its lower melt viscosity. Similar to the samples of which PP is the dispersed phase, the clay is mainly distributed in the interface areas as aggregates of clay layers in $\sim$1 μm long along the interface, which is consistent with the observations from the SEM images of j and k in Figure 1. In addition, there are tactoids are noticed in the PTT domains, but no clay is discerned in the PP matrix. It confirms the viewpoint that the clay has higher affinity with PTT than PP, and it prefers to locate at the interfaces or in the PTT phase for keeping the lowest energy rule.

Although the images in Figure 5 show that the clay is mainly distributed in the interface areas along the borderlines and the rest is located in the PTT domains, no matter PTT is as the dispersed phase or the matrix, its effects on the phase morphology are different. To elucidate the mechanism, it is necessary to consider the three processes occurred simultaneously during the mixing process. One is the dispersion-coalescence process of the dispersed phase in the matrix, which is influenced by the presence of clay, the relative viscosity ratio of the melts, and the interfacial tension. The other is the two intercalation processes of PTT and PP into the clay galleries, which occur separately in their domains or at the phase interfaces. The intercalation/exfoliation feasibility is mainly determined by the affinity between the clay and the polymers. Another is the process of the clay transferring from one polymer domain to another polymer domain and/or to the phase interfaces, which is driven by the different affinities between the clay and the two polymers, and eventually results in a selective distribution in the two polymers. Considering the overall results of WAXD, SEM, and TEM, it is suggested that the hydrophobicity of clay is between those of the two polymers, and the clay would rather to transfer to the phase interfaces for keeping lower energy. Moreover, the transfer speed of clay from the PP domains is faster than that from the PTT domains owing to its higher affinity with PTT than PP. As a result, not all the clay in the PTT domains can finish the transfer process in the limited mixing time, whereas the mixing time is enough for the clay in the PP phase to fulfill the transfer process. Therefore, when PTT is the matrix phase, the coalescence of the PP phase was retarded by the presence of clay with the high aspect ratio in the matrix and resulted in fine morphologies. For the cases of where PP is the matrix phase, the remained clay in the PTT domains and the clay at the interfaces make the viscosity of the PTT phase be increased because of its high aspect ratio, thus the viscosity ratio between the PTT phase and the PP phase change. At the same shear, the dispersion of the PTT phase becomes more difficult than the corresponding system without clay, so the dimension of the dispersed PTT domains is a little larger than the cases of without clay.

CONCLUSIONS

PTT/PP/MMT nanocomposites were prepared via melt compounding. When PP is the dispersed phase, the clay plays an important role in reducing the domain size of the PP phase, but no improvement of the interface adherence is observed during the finer dispersion development of the PP phase. When PP is the matrix phase, the dimension of the dispersed PTT phase is a little larger in the presence of 2 wt % clay compared with the case of without clay. TEM observations indicate that clay is mainly distributed at the phase interfaces along the phase borderlines. In addition, some intercalated clay tactoids (multilayer particles) are observed in the PTT matrix whereas no discernable clay particles can be found in the PP phase, indicating that the clay has higher affinity with PTT than PP. In the presence of 5 wt % PP-g-MAH, the dispersed domains distribute rather uniformly in the matrix with excellent interface adherence, and most clay is exfoliated and distributed at the interfaces forming phase borderlines in polygonal shape.

We thank the financial supports from the Natural Science Foundation of Shandong Province, China, for Excellent Youth Scientists (No. 2008BS04006), and the Open Foundation of Key Lab of Rubber-Plastics, Ministry of Education, Qingdao University of Science & Technology.

References

1. Hale, W.; Keskkula, H.; Paul, D. R. Polymer 1999, 40, 365.

2. Wang, C.; Su, J. X.; Li, J.; Zhang, Q.; Yang, H.; Du, R. N.; Fu, Q. Polymer 2006, 47, 3197.
3. Xue, M. L.; Sheng, J.; Chuah, H. H.; Zhang, X. Y. J Macromol Sci Phys 2004, 43, 1045.
4. Li, X. C.; Kang, T. K.; Cho, W. J.; Lee, J. K.; Ha, C. S. Macromol Rapid Commun 2001, 22, 1306.
5. Perrin-Sarazin, F.; Ton-That, M. T.; Bureau, M. N.; Denault, J. Polymer 2005, 46, 11624.
6. Wang, K.; Deng, J. N.; Yang, H.; Zhang, Q.; Fu, Q.; Dong, X.; Wang, D. J.; Han, C. C. Polymer 2006, 47, 7131.
7. Ray, S. S.; Bousmina, M. Macromol Rapid Commun 2005, 26, 450.
8. Li, Y. J.; Shimizu, H. Macromol Rapid Commun 2005, 26, 710.
9. Khatua, B. B.; Lee, D. J.; Kim, H. Y.; Kim, J. K. Mcaromolecules 2004, 37, 2454.
10. Zou, H.; Zhang, Q.; Tan, H.; Wang, K.; Du, R. N.; Fu, Q. Polymer 2006, 47, 6.
11. Tang, Y.; Hu, Y.; Zhang, R.; Gui, Z.; Wang, Z. Z.; Chen, Z. Y.; Fan, W. C. Polymer 2004, 5317.
12. Feng, M.; Gong, F. L.; Zhao, C. G.; Chen, G. M.; Zhang, S. M.; Yang, M. S. Polym Int 2004, 53, 1529.
13. Wu, J.; Schultz, J. M.; Samon, J. M.; Pangelinan, A. B. Polymer 2001, 42, 7141.
14. Grande, J. A. Mod Plast 1997, 12, 97.
15. Jeong, Y. G.; Woo, J. B.; Won, H. J. Polymer 2005, 46, 8297.
16. Xue, M. L.; Yu, Y. L.; Chuah, H. H.; Qiu, G. X. J Macromol Sci Phys 2007, 46, 387.